Journal of Asian Earth Sciences 249 (2023) 105619

Contents lists available at ScienceDirect

Journal of Asian Earth Sciences

journal homepage: www.elsevier.com/locate/jseaes

3D seismic tomography models of the Baikal Rift zone and surrounding areas based on regional seismological data

Irina Medved [a,b,c,*], Viktoria Komzeleva [b,c], Ivan Koulakov [c,d], Mikhail Buslov [a], Alena Filippova [e,f]

[a] Sobolev Institute of Geology and Mineralogy SB RAS, Koptyug Ave., 3, 630090 Novosibirsk, Russia
[b] Novosibirsk State University, Pirogova st.,2, 630090 Novosibirsk, Russia
[c] Trofimuk Institute of Petroleum Geology and Geophysics SB RAS, Koptyug Ave., 3, 630090 Novosibirsk, Russia
[d] Institute of the Earth's Crust SB RAS, Lermontova St., 128, 664033 Irkutsk, Russia
[e] Pushkov Institute of Terrestrial Magnetism, Ionosphere and Radio Wave Propagation of RAS, Kaluzhskoe shosse, 4, 142190 Troitsk, Russia
[f] Institute of Earthquake Prediction Theory and Mathematical Geophysics RAS, Varshavskoe Shosse St., Kor. 2, 79, 113556 Moscow, Russia

ARTICLE INFO

Keywords:
Baikal Rift Zone
Collision zone
Seismic tomography
Neotectonics
Geodynamics
Rift zone
Eastern Sayan
Siberian Platform
Crustal structure

ABSTRACT

We present seismic tomography models of the Baikal Rift Zone (BRZ), obtained from regional seismological data recorded in the period 1994–2016. 3D models of P- and S-wave velocity distributions under the BRZ were built down to a depth of 60 km with the LOTOS local seismic tomography algorithm. An overall picture of the heterogeneities coincides with the already existing ideas on the seismic structure of the region: a high-velocity anomaly in the north corresponds to the Siberian Craton; low-velocity anomalies in the western part of the study area are apparently due to the presence of the Cenozoic plume; the Baikal Rift Zone is characterized by a low-velocity anomaly down to a depth of 35–50 km, which accords with the present-day concepts of the Moho discontinuity depth. Moreover, below the BRZ there is a jump in the lower boundary of the low-velocity anomaly, which is in line with the Moho jump recognized in the existing investigations. In addition, based on the results obtained, we identified a number of heterogeneities not revealed earlier. For example, high-velocity near-surface anomalies in the Middle Baikal block, which were interpreted as heavy gabbro-metagabbro bodies, displaced as a result of the Cenozoic strike-slip. Based on the results obtained, as well as on the review of the existing geological and geophysical works, the authors argue in favor of a passive model during the formation of the Baikal Rift.

1. Introduction

The Baikal Rift Zone (BRZ) is one of the largest neotectonic rift systems in the world (Dobretsov et al., 2021; Jolivet et al., 2013; Levi et al., 1995, 1997; Logachev, 1999, 2003; Lunina et al., 2010; Zonenshain et al., 1992; and many others). It is located in the junction zone of the Siberian Platform and northern part of the Central Asian Fold Belt (Amur Plate) (Fig. 1). The energy sources for the BRZ formation are believed to be: 1) asthenospheric diapir (Kulakov, 2008; Logatchev and Zorin, 1987; Windley and Allen, 1993; Zorin, 1981), 2) mantle plume (Petit et al., 2008; Tiberi et al., 2003), 3) long-range impact of the Indo-Eurasian collision (Davy and Cobbold, 1988; Delvaux et al, 1997; Dobretsov et al., 1995, 1996; Fournier et al., 1994, 2004; Jolivet et al., 1990, 1992; Kimura et al., 1990; Molnar and Tapponnier, 1975; Petit et al., 1996; Petit and Deverchere, 2006), or a combination of the local and remote sources (Chemenda et al., 2002; Lebedev et al., 2006; Lesne et al., 2000; Logachev, 2003; Zorin et al., 2003; Zorin and Turutanov, 2005).

There exist several main arguments in favor of the models 1 and 2. The first argument is the existence of a regional uplift of the BRZ, which reaches 3,000 m on the flanks and 1,500 m in the middle part (Logatchev and Zorin, 1987). The second argument is the increased heat flow: in the BRZ region it is higher than at the Siberian Platform (35–45 mW/m^2) and Eastern Sayan (55–65 mW/m^2), and has a high differentiation (40–50 mW/m^2 – 300 mW/m^2) (Duchkov & Sokolova, 2014; Lysak, 1984; Tiberi et al., 2003). The third argument is the occurrence of the Cenozoic basaltic magmatism (Kiselev et al., 1978; Rasskazov et al., 2002).

* Corresponding author at: Institute of Geology and Mineralogy SB RAS, Koptyug Ave., 3, 630090 Novosibirsk, Russia.
E-mail address: Zabelirina@yandex.ru (I. Medved).

https://doi.org/10.1016/j.jseaes.2023.105619
Received 7 June 2022; Received in revised form 10 December 2022; Accepted 8 March 2023
Available online 15 March 2023

The geomorphology of mountain systems in Central Asia and its neotectonic structure began to be considered as the result of intercontinental deformations associated with the distant impact of tectonic stress from the Indo-Eurasian collision (Molnar and Tapponnier, 1975). Later it was established that the presence of such large 'rigid' Precambrian blocks in the structure of the Central Asian Fold Belt as the Tarim, Central Tien Shan (Issyk-Kul), Tuva-Mongolian and others contributed to the transfer of tectonic stresses over long distances up to several thousand kilometers from the Indian to the Siberian continent (Buslov et al., 2007, 2008; De Grave & Buslov, 2007; Dobretsov et al., 1996, 2013, 2016, 2019). This process is believed to have been facilitated by numerous plumes, above which heated parts of the lithosphere might have been subjected to folding and strike-slip displacements. The displacement vectors derived from GPS results (e.g. Calais et al., 2003; Flesch et al., 2001) and from mathematical modeling (Sobolev et al., 2005) fairly well describe the formation of the BRZ due to plate movement resulting from the Indo-Eurasian collision.

There are two stages singled out in the BRZ formation: 'slow rifting', which lasted from the Oligocene to the late Miocene (30–5 Ma) (Bazarov, 1986; Logachev, 2003; Mashchuk and Akulov, 2012; Rasskazov et al., 2014; Zonenshain and Kazmin, 1995; and many others), and 'rapid rifting', which began about 5 Ma (Artyushkov, 1993; Buslov, 2012; Nikolaev et al., 1985; Petit and Deverchere, 2006). The first stage is described by a slow subsidence of basins with the accumulation of fine-grained sediments against the background of a general domal uplift of the region. The last stage involves an increase in the sinking rate of the basins, especially those of Baikal, the accumulation of thick coarse deposits in them, and the intensification of orogenic processes in adjacent ridges.

Thus, there are a large number of works aimed at identifying the causes of active tectonics in the BRZ, which is largely related to the deep structure features. In this connection, seismic tomography remains one of the main geophysical techniques for studying the deep structure, its approaches being able to reveal various features of the region. For instance, the receiver function and deep seismic sounding methods help identify the Moho discontinuity with high accuracy. Estimates for the Moho depth under the study region differ, but common features can be identified. Specifically, the thickness of the Earth's crust under the Siberian Platform is within 35–40 km (e.g. Gao et al., 2004; Krylov et al., 1981; Mordvinova et al., 2019; Zorin et al., 2002), the thickest crust (44–55 km) is located under the mountain structures of the Eastern Sayan and Khamar-Daban (Gao et al., 2003; Laske et al., 2013; Mordvinova et al., 2019; Vinnik et al., 2017), whereas under the South Baikal block the Moho reaches 30–35 km (Vinnik et al., 2017; Zorin et al., 2003). In general, a thinning of the crust under Baikal is noted by both deep seismic sounding specialists (Krylov et al., 1981; Suvorov et al., 1999, 2002) and those dealing with receiver functions (e.g. Gao et al., 2004; Vinnik et al., 2017; Zorin et al., 2002). The sedimentary layer is practically absent under the inter-basin mountain barriers, having a thickness of 1 to 10 km under the rift basins and reaching its maximum thickness under the South Baikal basin (Hutchinson et al., 1992; Krylov et al., 1981; Nielsen and Thybo, 2009; Scholz et al., 1993; Ten Brink and

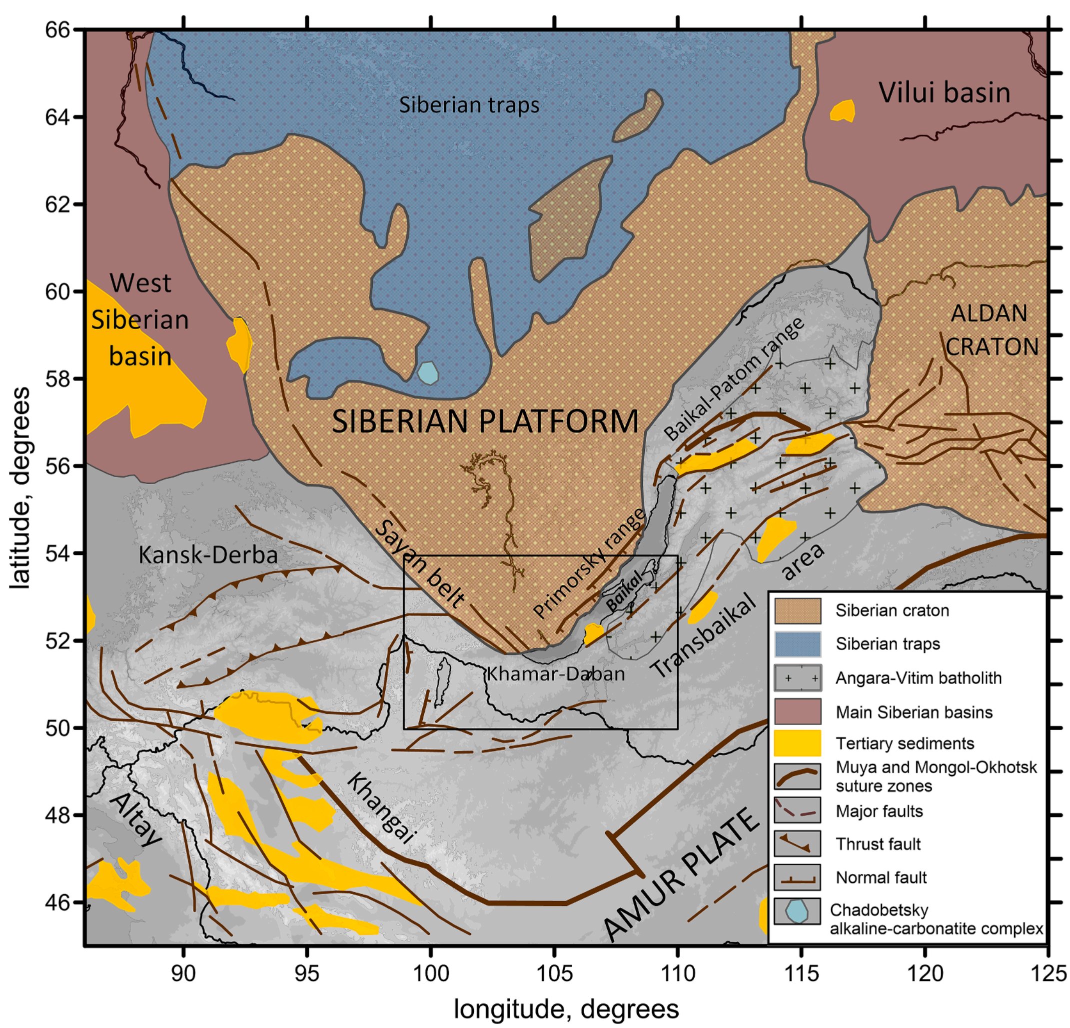

Fig. 1. Location of the study region (black box) relative to large geologic and tectonic objects. The map is based on Jolivet et al. (2013).

Taylor, 2002; Song et al., 1996).

Concerning the Baikal region, there have been a number of seismic tomography investigations of regional (Koulakov et al., 2002; Kulakov, 1999; Mordvinova et al., 2000; Seredkina et al., 2016; Tiberi et al., 2003; Wu et al., 2021; Zhao et al., 2006) and local scales (Kulakov, 1999; Petit et al., 1998; Yakovlev et al., 2007). The advantage of seismic tomography for the Baikal region is that it enables tracing the features of the deep structure for a larger area as opposed to the deep seismic sounding and receiver function methods. The regional tomography works (Kulakov, 2008; Mordvinova et al., 2000; Tiberi et al., 2003; Zhao et al., 2006) exhibit similar features: high velocities at the Siberian Platform, and low-velocity areas for the upper mantle at the Baikal basins and mountain uplifts of the region. As for the local tomography, negative anomalies under the southwestern part of the BRZ correlate with the Late Cenozoic volcanic fields.

Seismic tomography allows for obtaining sufficiently detailed 3D images of a deep seismic structure in some region to trace its geodynamic mechanisms. The ever-evolving seismic data analysis and inversion techniques, along with other geophysical and geological data, can help researchers move from assumptions caused by gaps in a deep structure to more definitive conclusions when solving geodynamic problems. The novelty of the presented study lies in the use of unique data, through which we obtained high-resolution seismic tomography results. We reviewed the influence of structural and compositional characteristics of the Baikal basement on the formation of its structure as a result of regional compression from the Indo-Eurasian collision.

1.1. The BRZ geology and structure

The main Cenozoic tectonic units of the BRZ are depicted in Fig. 2. The BRZ comprises many rift basins and faults, which are a complex active system (Jolivet et al., 2013; Levi et al., 1995, 1997; Logachev, 1999, 2003; Lunina et al., 2010). Many BRZ faults were found to have a strike-slip component, but it is normal faults that predominate in the central and northeastern segments (Jolivet et al., 2013; Rasskazov et al., 2010). According to the map of faults for southeastern Siberia and the corresponding database (Lunina et al., 2010), the data indicate that normal faults predominate in active fault segments in the study area, with downdip-strike slip playing a minor role. Along the western flank of the lake in the north–south direction, predominant are normal faults and left lateral strike slip-downdip faults.

The BRZ is located in the Early Paleozoic Olkhon strike-slip zone, separating the Siberian Craton from the Central Asian Fold Belt. The zone is composed of a complex of diverse igneous and metamorphic rocks and represents a series of linear tectonic slabs (Fig. 3) formed during frontal and oblique collision between the Central Asian Folded Belt structures and the Siberian Craton. There are several stages of tectogenesis (thrusting, domal, strike-slip), accompanied by high-temperature metamorphic transformations along with basic and granitoid magmatism. The degree of metamorphism within the strike-slip zone varies from the granulite to amphibolite and epidote–amphibolite facies (Donskaya et al., 2017; Fedorovskii et al., 2019, 2005, 1995; Fedorovsky and Sklyarov, 2015; Sklyarov et al., 2020).

A characteristic feature of the granulite zone is its saturation with gabbroid bodies (more than 150) (Dobretsov, 2020; Vladimirov et al., 2017). The latter have sharp contacts with host mafic granulites, gneisses and quartzites, and less often marbles. One can encounter gabbroid massifs up to many tens of kilometers long (Fig. 3), with garnet being often found in the gabbroids. Drawing from the structure and composition of the constituent minerals, these rocks are identified as eclogite-like (Dobretsov, 2020).

2. Data and method

In order to obtain models for velocity anomalies distribution, we used the arrival times of P- and S-waves from 4,000 earthquakes recorded by 102 seismological stations over the 1994 to 2016 period. A total of 100,783 rays were employed: 45,634P-wave and 55,149 S-wave rays. The stations belong to the Baikal, Altai-Sayan, Buryat, Yakut, and Mongolian permanent regional seismic networks. The main accumulation of the earthquake sources occurs at depths of 5–25 km, which coincides with somewhat variable estimates obtained in the studies

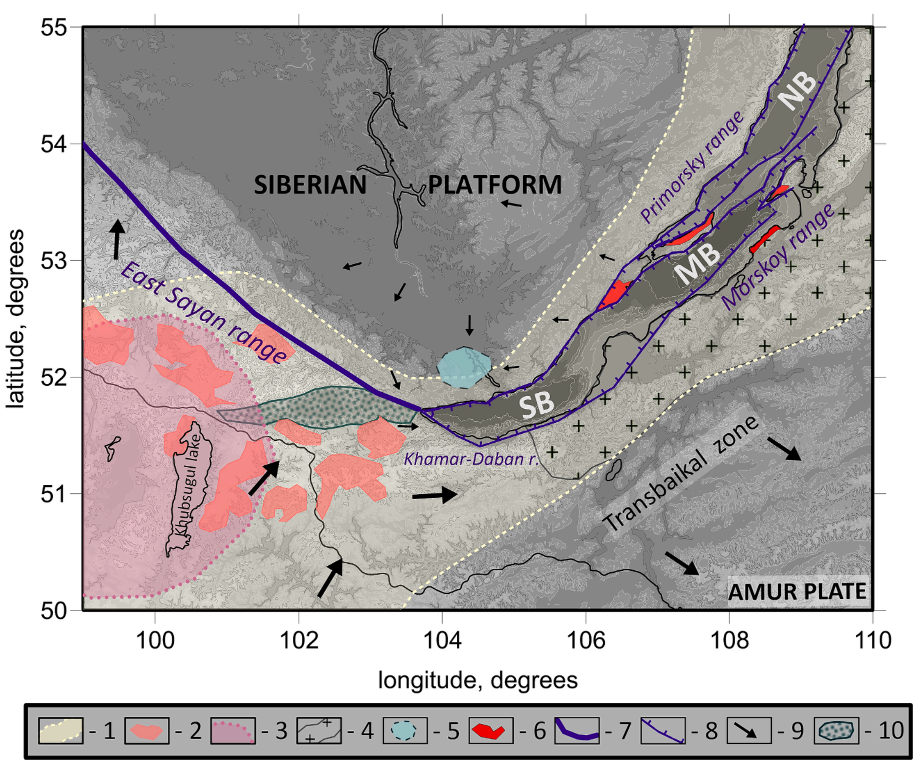

Fig. 2. Map of plates and tectonic structures of the Baikal Rift Zone and surrounding areas with additions (Zorin et al., 2003). Abbreviations: SB – South Baikal rift basin, MB – Middle Baikal rift basin, NB – North Baikal rift basin. Legend: 1 – Baikal Rift Zone; 2 – magmatic fields; 3 – Sayan-Baikal domal uplift (Zorin et al., 2003); 4 – Angara-Vitim batholith (Dobretsov et al., 2019); 5 – presumed igneous rocks similar to the Late Permian-Early Triassic Chadobets alkaline-carbonatite complex; 6 – gabbro and metagabbro (Dobretsov, 2020); 7 – Main Sayan fault; 8 – active normal faults of Lake Baikal (Jolivet et al., 2013; Lunina et al., 2010); 9 – directions of contemporary crustal movements reported by GPS data (Lukhnev et al., 2010); 10 – Tunka basin.

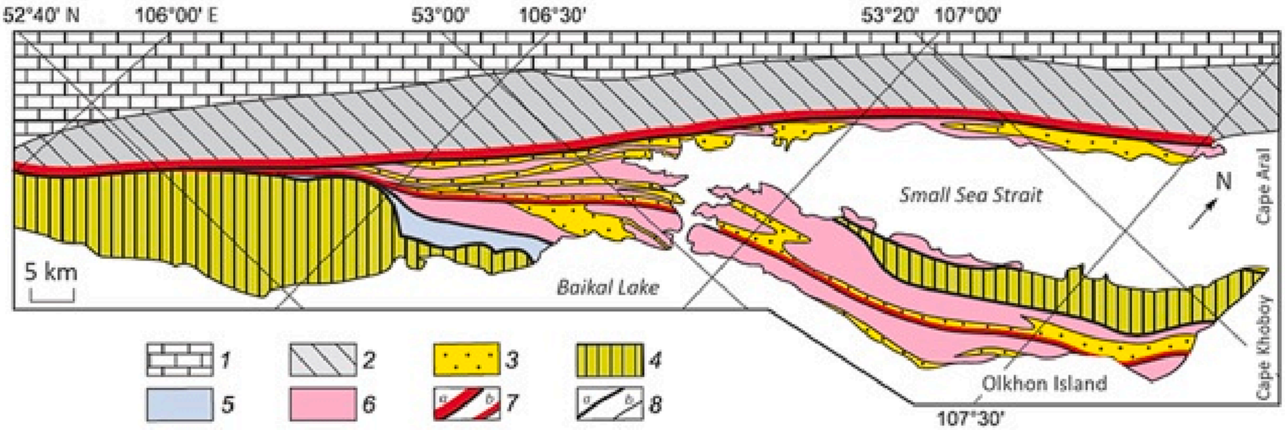

Fig. 3. Tectonic scheme of the Olkhon collisional system according to Fedorovsky et al. (2010). Legend: 1, 2 – Siberian continental plate: 1 – Riphean-Paleozoic slightly deformed sedimentary cover; 2 – plate basement formed by the Paleoproterozoic metamorphites and granites; 3–6 – Early Paleozoic Olkhon collisional system (combination of strike-slip plates of different composition and age): 3 – plates formed by a metamorphic complex with variegated composition involving gabbroids (500 Ma); 4 – plates formed by a metamorphic complex with variegated composition involving gabbroids (500 Ma) (granulite metamorphic facies); 5 – plate formed by the Orso amphibolite complex; 6 – plates formed by granite-gneisses and migmatites of the Shebarta complex (460–470 Ma) with signs of the Archean and Paleoproterozoic protolith; 7a – collisional suture (boundary between the Siberian Craton and Olkhon collision zone; blastomylonites after the craton and terrane rocks, outliers of the Paleozoic granulites among blastomylonites); 7b – main strike-slip zone; 8a – blastomylonite zones between groups of various-type strike-slip slabs; 8b – blastomylonite zones between individual strike-slip slabs.

(Golenetsky & Perevalova, 1988; Gileva et al., 2000; Melnikova et al., 2010; Radziminovich, 2010; Suvorov et al., 2008). According to the calculation data on bulk and regional depth–frequency distributions of the earthquakes by Déverchère et al. (2001), the earthquakes were shown to occur up to a 35–40 km depth.

Prior to inverting the data, we rejected the events with a total number of P- and S-picks less than 7. Afterwards, the data catalog included 2,196 earthquakes and 70 stations. The number of rays equaled almost 40,000: ~20,000P-wave rays and ~ 19,000 S-wave rays (an average of 18 picks per event). The observation network is plotted in Fig. 4.

The tomographic inversion was performed by means of the LOTOS

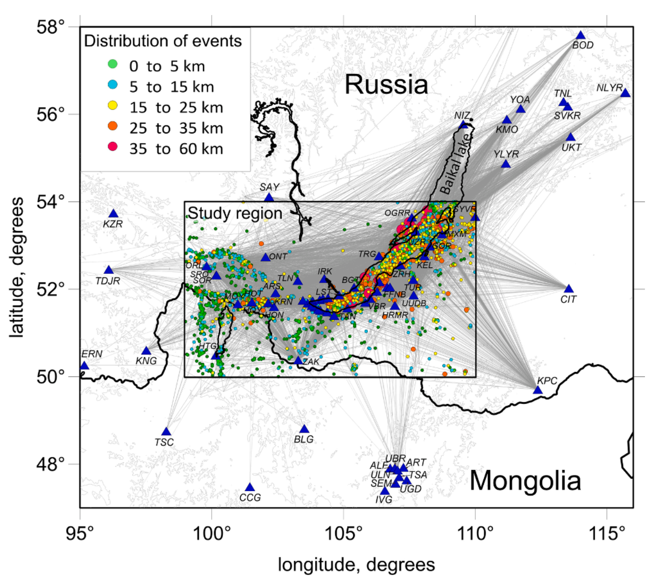

Fig. 4. Earthquakes and seismological stations map. The map shows the distribution of P- and S-wave ray paths (grey lines) and seismic stations (blue triangles). Multi-colored dots indicate the distribution of earthquakes by depth. In the south of Lake Baikal there are stations (unsigned): BAN, BBA, BBK, BBN, BBT, BMN, BMR, BMU, BRH, BSA, BTU, BUT. (For interpretation of the references to colour in this figure legend, the reader is referred to the web version of this article.)

(Local Tomography Software) nonlinear algorithm, which provides simultaneous inversion of P- and S-velocities and source coordinates. Theoretical concepts and technical details of the algorithm are described in detail in Koulakov (2009).

At the first stage, the user defines a 1D reference velocity model; for the current investigation it is given in Table 1. The model was selected on the basis of the existing seismic tomography studies of the BRZ through the LOTOS algorithm (e.g. Kulakov, 1999; Yakovlev et al., 2007). In the 1D reference model, the velocities between the given depths are linearly interpolated. Further, a preliminary estimation of the sources' coordinates is carried out via the grid search method. For this step, one needs to set such parameters as, for example, the minimum allowable number of registered phases per event, the maximum distance to the nearest station, etc.

At the next step, the sources are localized within a 3D velocity model. To calculate the wave travel times, a ray-tracing algorithm is applied. It is centered around the ray path winding method for the rays propagating in the medium with the shortest time (Fermat's principle) (Um and Thurber, 1987). The algorithm for determining the most probable source locations is based, similarly to the 1D case, on finding the target function extremum. However, the grid search method is too labor-consuming for 3D ray tracing, so it the gradient descent method that is utilized to provide fairly rapid calculations.

After that, the algorithm proceeds to the construction of a parameterization grid in order to obtain a 3D distribution of velocity anomalies. The nodes of this grid are allocated in the studied volume according to the ray density. In the absence of rays, no nodes are created, and neither is inversion done in such areas. Between the nodes, the velocity is approximated linearly. To reduce the grid geometry effect on the results, four grids with different orientations (0, 22, 45 and 66 degrees) are

Table 1
1D reference model.

Depth, km	Vp, km/s	Vs, km/s
−5.0	5.9	3.37
10.0	6.5	3.71
25.0	6.9	3.94
43.0	7.8	4.45
77.5	8.04	4.59
120.0	8.2	4.68

inverted, and then the results are averaged into a single model. The algorithm ensures simultaneous inversion of source parameters, P- and S-wave anomaly distributions, and station corrections.

Matrix inversion is performed by the LSQR method (Nolet, 1987; Paige and Saunders, 1982). Its stability is regulated by amplitude damping and smoothing, which are reduced to minimizing velocity anomaly differences in neighboring nodes. The LOTOS code allows adjusting anomaly amplitudes and smoothing in both vertical and horizontal directions. The optimum values for the smoothing coefficients, together with the weighting factors for the station and source corrections, were determined after several numerical calculations. Next, several iterations are executed, each including the stages of hypocenter refinement, matrix calculation and inversion. In total, we did five iterations; the mean residual deviations were reduced from 0.48 s to 0.35 s (27%) for the P-wave data and from 0.76 s to 0.47 s (38%) for the S-wave data.

3. Models and tests

The main results of the local tomography are 3D models of P- and S-wave velocity anomalies presented in horizontal sections at depths of 5, 10, 20, 40 and 50 km (Fig. 5), as well as in five vertical sections (Fig. 6). Before interpreting the results, it is necessary to have an idea about the reliability of the observation network resolution.

To understand the resolution, there exist several arguments that should be taken into consideration as early as at the stage of obtaining the first models.

The first argument in favor of the reliability of seismic tomography results is similar structures of P- and S-wave velocity anomalies. Regarding the horizontal models obtained in this work, the P and S anomalies have similar configurations, but they diverge mainly in the southern and southeastern parts of the study region. Thus, for instance, one should be meticulous about the linear high-velocity anomaly located in the southern part of Lake Baikal in the area of the Selenga River, shown in the horizontal sections at 5 and 10 km. This high-velocity anomaly is present in the P-models and absent in the S-models. The same applies to the high-velocity anomalies in the southeastern part of Lake Baikal, apparent in the P-models only. The observed inconsistencies are associated with insufficient ray density in the southeastern part of the considered region. This can be observed in Fig. 4 showing the earthquake distribution and ray density. Therefore, the observed inconsistencies in this area are most likely related to artifacts.

The second argument is the correlation of the observed anomalies with large geological objects, such as tectonic blocks, large faults and vast sedimentary basins. According to Fig. 5, at all the depths there is a good correlation between the large high-velocity anomaly in the north of the region under investigation and the Siberian Platform basement. The linear low-velocity anomalies passing along Baikal as well as anomalies outlining the Siberian Craton are most likely to belong to fault structures. In general, the BRZ in our tomography models is distinguished as a low-velocity structure, which reflects its fragmentation and decompaction relative to the Siberian Platform.

Fig. 7 shows a synthetic checkerboard test with reconstructed models for 40 × 40, 40 × 40, 60 × 60 and 80 × 80 km anomaly sizes at depths of 5, 10, 30 and 50 km respectively. The amplitude of the positive and negative anomalies is ± 5%. The anomalies change sign both laterally and in depth. The synthetic test revealed the resolution of the observation network to be capable of reconstructing 40 × 40 km structures in horizontal sections at 5 and 10 km depths underneath Lake Baikal and in a small area below the Eastern Sayan. This is due to the highest ray density there, which is well demonstrated in Fig. 4. At a depth of 30 km, 60 × 60 km anomalies are optimally reconstructed both in the eastern and western parts of the region, while poor resolution is still observed in its north and south. The checkerboard 80 × 80 km anomalies were reconstructed throughout almost the entire territory to a depth of 50 km, but the southeastern part is still poorly resolved. All the models exhibit smearing of the anomalies from the southwest to northeast, which is associated with the ray configuration. Based on the conducted test, we conclude that the resolution is not uniform: under Lake Baikal and the Eastern Sayan small 40 × 40 km anomalies can be resolved. By contrast, in the Siberian Craton area the anomalies to be restored should be 80 × 80 km at least.

Fig. 8 gives a synthetic test with realistic anomalies in the vertical section BB' down to a depth of 60 km. The synthetic anomalies presented in Fig. 8.c were set in accordance with those observed in the basic model. The result of solving for the synthetic model is in Fig. 8.b. In carrying out this test, we pursued several goals. First, to identify near-surface high-velocity anomalies under the BRZ – are they really recoverable with the existing ray configuration? Second, to determine whether there is a sedimentary cover under Baikal, which is present to 10 km depth as indicated by Nielsen and Thybo (2009). In seismic tomography, such a large sedimentary cover should appear as a low-velocity anomaly, but this is not the case in our results. On the contrary, in the models obtained there is a high-velocity anomaly under Baikal. In this connection, we preset a low-velocity anomaly with ~ 10 km depth in the synthetic model under Baikal (Fig. 8.c). Following the inversion results (Fig. 8.b), the specified low-velocity anomaly in the area of the Irkutsk Reservoir does not manifest itself.

4. Discussion and interpretation

4.1. General picture of heterogeneities

A general picture of the obtained distribution of seismic velocity anomalies corresponds to the geological setting of the region. As it appears from the horizontal sections presented in Fig. 5, the ancient Siberian Craton stands out in the form of a high-velocity anomaly, while lower seismic wave velocities predominate in the crust under the BRZ. Noteworthy that, in general, the low-velocity anomaly fits well within the boundaries of the BRZ by Zorin et. al., (2003), which are highlighted in Fig. 5 by the dash line. According to the profile EE' (Fig. 6.), built along Lake Baikal, the large low-velocity anomaly is characterized by heterogeneity and a thickness of 35 to 40 km. However, according to the vertical sections BB', DD' (Fig. 6) across the strike of Baikal, the thickness of the low-velocity anomaly reaches 50 km in some places and has an increase trend under the southeastern shore of Baikal, under Khamar-Daban. The Baikal Rift Zone, relative to the surrounding geological units such as, for example, the Siberian Craton, is mechanically weakened, since it is represented by numerous faults and is filled with sediments. Therefore, the presence of the low-velocity anomaly under the BRZ is quite natural. Of particular interest is the lower boundary of this anomaly. Due to the technical features, the local tomography method does not allow detecting boundaries. However, in fact, in some works carried out with the LOTOS code, a correlation was recorded between anomaly boundaries and the Moho discontinuity obtained by the receiver function method. For example, in Koulakov et al. (2014) and Medved et al. (2022) the lower boundary of the seismic velocity anomaly constructed via LOTOS corresponds to the Moho discontinuity under the Himalayas from receiver functions. In the present study, the lower boundary of the low-velocity anomaly under Lake Baikal occurs at depths of about 35 to 50 km, which agrees with the Moho discontinuity data in the BRZ region (Gao et al., 2003; Laske et al., 2013; Mordvinova et al., 2019; Vinnik et al., 2017). Moreover, on profiles BB' and DD' in Fig. 6 one can see a jump in the lower boundary of the low-velocity anomaly beneath Lake Baikal, which is attributable to the Moho jump pointed out in Zorin et al. (2003). The Moho jump is marked by the black dash line in Fig. 6. An important conclusion of this work is that this jump is traced both under the southern and under the Middle Baikal block, which is clearly seen on profiles AA', BB' and DD' in Fig. 6. This feature is also clearly visible on the 40 km horizontal section in Fig. 5, where linear high-velocity anomalies stand out under the South and Middle Baikal block; along the northwestern and southeastern shores of Baikal

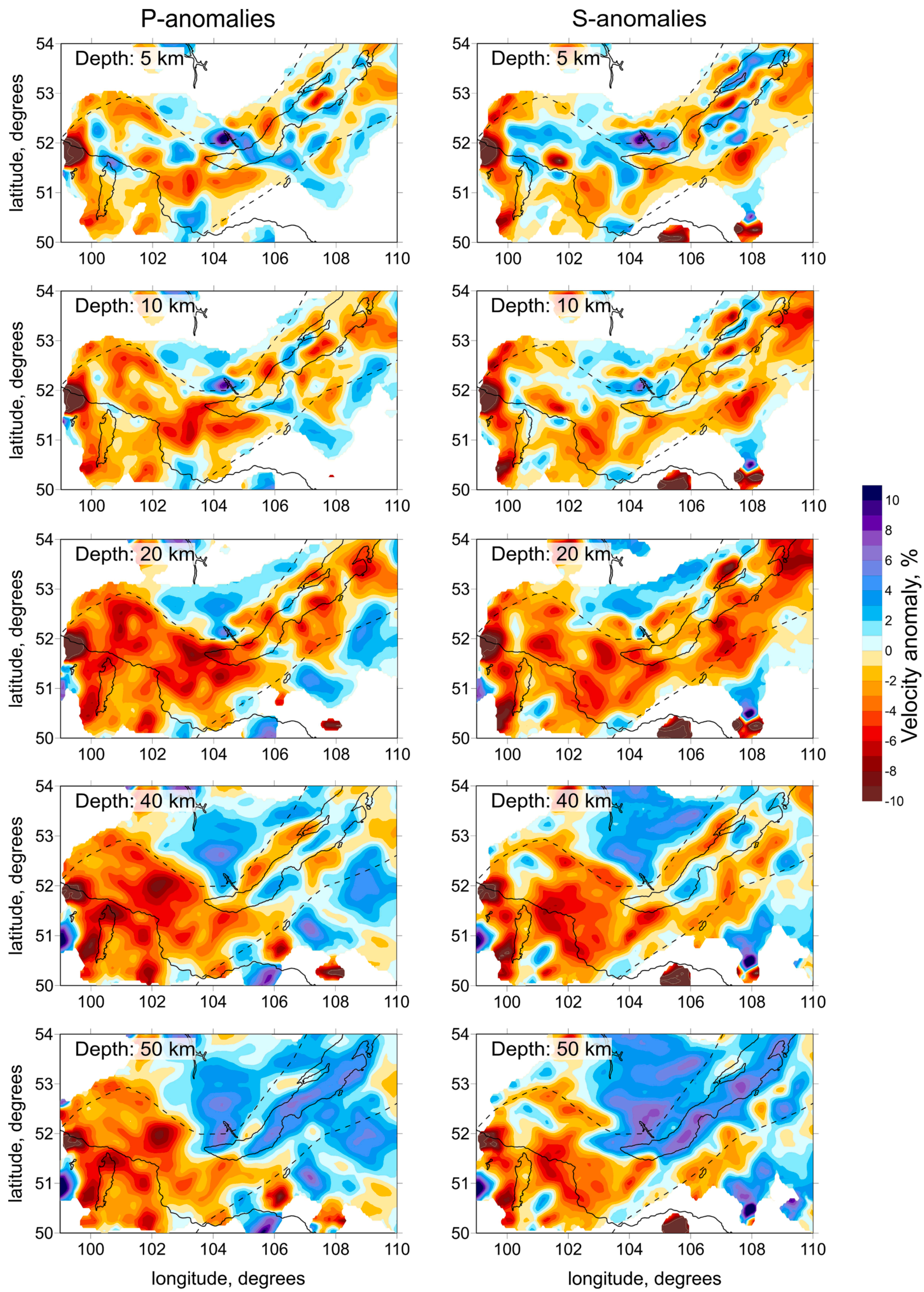

Fig. 5. P- and S-wave velocity anomalies in horizontal sections at depths of 5, 10, 20, 40 and 50 km. The dashed line marks the BRZ boundaries by Zorin et al. (2003).

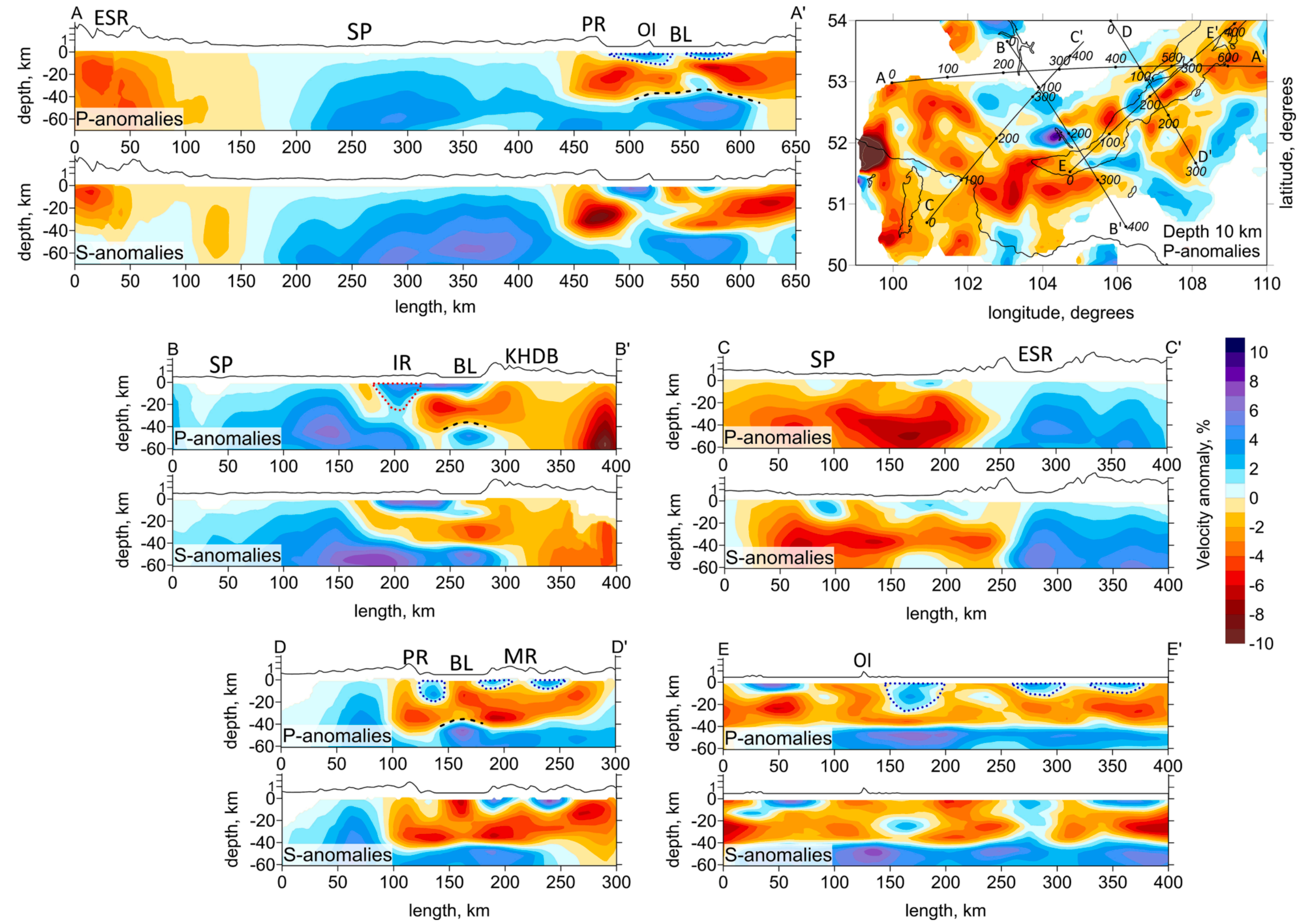

Fig. 6. P- and S- velocity anomalies in four vertical sections. The location of the profiles is shown on the map for 10 km depth. Abbreviations: ESR – East Sayan range, SP – Siberian Platform, BL – Baikal Lake, OI – Olkhon Island, IR – Irkutsk Reservoir; KHDB – Khamar-Daban Range, MR – Morskoy Range, PR – Primorsky Range. The black line at the top of the vertical sections shows the topography; The black dash line shows Moho jump under Baikal Lake; The blue dotted line marks the supposed high-density metamorphosed eclogite-like rocks and gabbroids within the middle basin of Lake Baikal; The red dotted line marks the supposed ultramafic type rocks in the Irkutsk Reservoir area. (For interpretation of the references to colour in this figure legend, the reader is referred to the web version of this article.)

within the border of the BRZ by Zorin et al. (2003), there are low-velocity linear anomalies. The thinning of the low-velocity anomaly along Lake Baikal indicates that the crust is likely to be slightly thinned along the axis of the South and Middle Baikal block.

The Eastern Sayan region, located in the western part of the study area, stands out as a large low-velocity anomaly, which, according to the profile CC' (Fig. 6), can be traced throughout the entire crust. According to the results of seismic tomography (Kulakov, 2008; Seredkina et al. 2016, 2021; Wu et al. 2021), the mantle under the southwestern flank of the area is also characterized by low-velocity anomalies. Fig. 2 demonstrates the western part to be rich in manifestations of the Cenozoic magmatism. There exists a local uplift in the area of Lake Khubsugul, which may be a result of plume processes that are the cause of magmatism in the region of interest (Zorin et al., 2003). Data on the petrochemical systematics obtained by examining the geomorphological setting of different-age volcanic rocks on the western shore of Lake Baikal (Rasskazov et al., 2015) testify that the last eruptions occurred 18–12 Ma in the Tunka basin. As a rule, igneous bodies older than ~ 5 Ma are completely solidified and consolidated, and therefore they are conventionally distinguished in seismic tomography models as high-velocity anomalies. However, on the profile CC' (Fig. 6) the low-velocity anomaly underneath the Eastern Sayan is distributed all over the crust. Thus, we may assume that there is indeed a Khubsugul plume under the eastern part of the region under study, which heats up the crust and, thereby, causes a slowdown in seismic velocities in the crust.

4.2. Small near-surface anomalies

Starting a discussion on the interpretation of the small near-surface anomalies, it is worth noting that we will consider only those located within and near Lake Baikal. It follows from the ray distribution density in Fig. 4 as well as from the synthetic checkerboard test in Fig. 7 that the highest resolution of the observation network in the region involved takes place only there.

We draw special attention to the intense high-velocity anomaly in the Irkutsk Reservoir area well distinguished in the horizontal sections in Fig. 5 down to a 20 km depth and on the vertical profile BB' in Fig. 6. This feature was marked by the red dotted line in BB' in Fig. 6. It has an isometric shape with a diameter of up to 50 km and can be traced in the depth interval 5–30 km. The anomaly is located within the Siberian Craton (Fig. 1). The latter is represented by the Mesozoic sediments of the Irkutsk basin, which overlap a thick section of the Late Proterozoic–Paleozoic sedimentary rocks. To the north, on the right bank of the Angara River, one can discern the Late Permian–Early Triassic Chadobets alkaline-carbonatite complex of an isometric shape with a diameter of about 50 km (Chebotarev et al., 2017). The Chadobets complex consists of ultramafic rocks, picrites, carbonatites and kimberlites, many of which have a high density. It should be assumed that

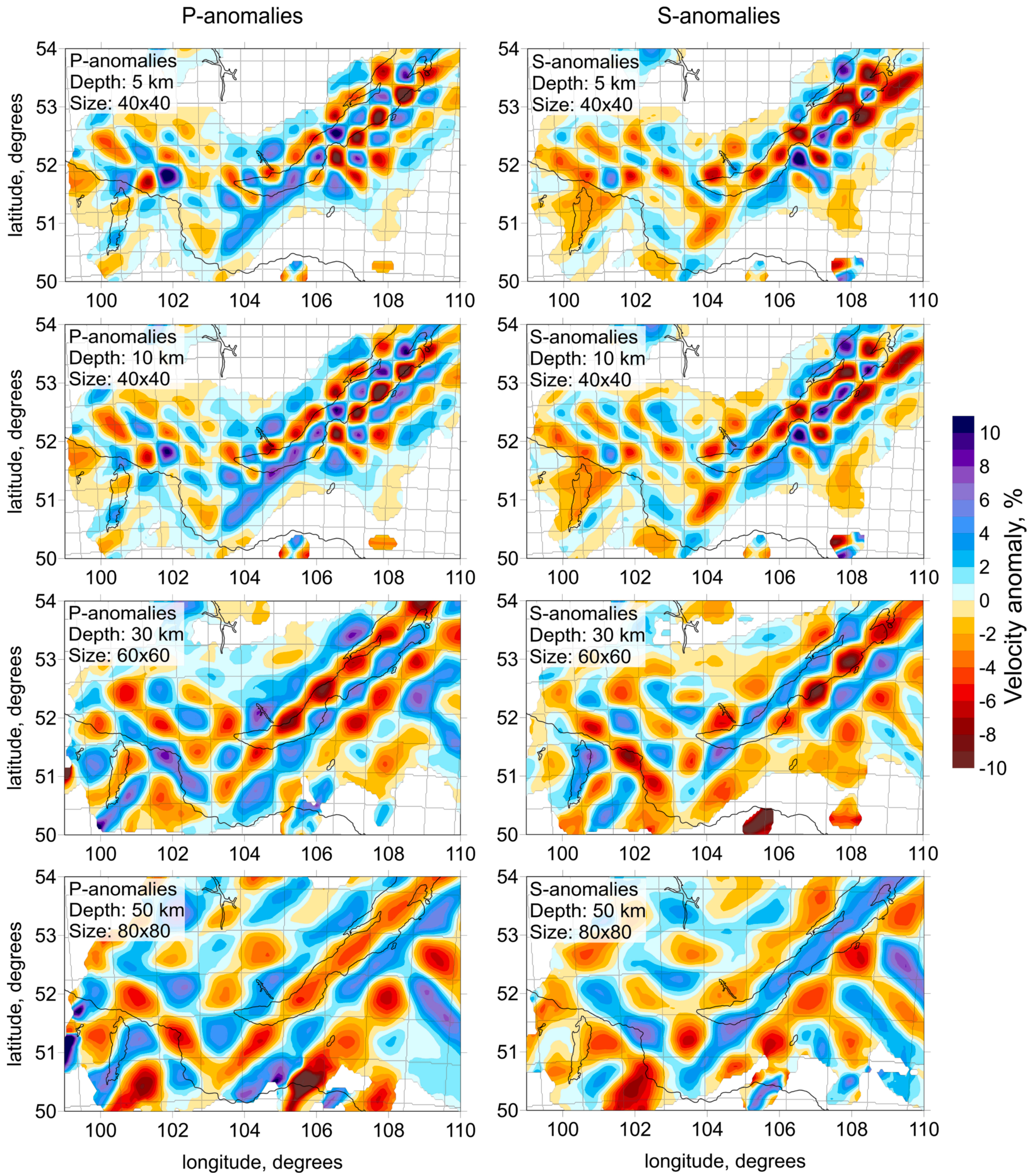

Fig. 7. Checkerboard test in horizontal sections for various sizes of anomalies: 40 × 40 km anomalies for 5 and 10 km depths, 60 × 60 km anomalies at 30 km and 80 × 80 km anomalies at 50 km.

the high-velocity anomaly in the Irkutsk Reservoir area, which is similar in shape and size, might correspond to this rock type.

Important structural features of the observed BRZ heterogeneities are the high-velocity anomalies within the middle basin of Lake Baikal. Their extreme northeastern part is intersected by the profile AA' (Fig. 6), whereon the anomalies have wedge-like shapes and they are traced back to a 20 km depth. On the profile DD' running at an angle of ~ 45 degrees to AA' (Fig. 6), there are high-velocity blocks below the Morskoy Range. The same peculiarities can be seen in EE' profile. The discussed high-velocity anomalies are marked by the blue dotted lines in Fig. 6. We suppose the high-velocity anomalies of the middle basin to be associated with the presence of high-density metamorphosed eclogite-like rocks

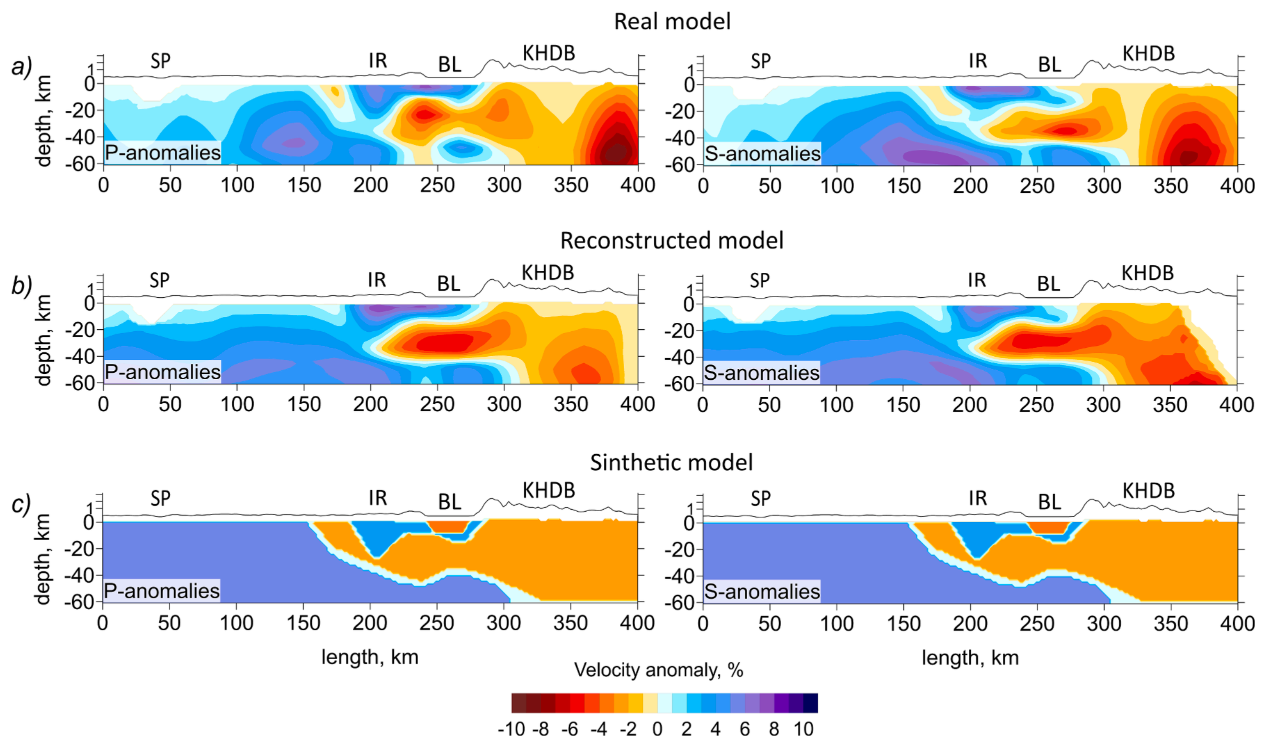

Fig 8. Synthetic test with realistic anomalies along the vertical section BB'. The profile location is shown in Fig. 4; variations in the day-surface topography are depicted above the profiles; a) real model obtained by the field data inversion; b) reconstructed synthetic model; c) synthetic model. Abbreviations: ESR – East Sayan range, SP – Siberian Platform, BL – Baikal Lake, OI – Olkhon Island, IR – Irkutsk Reservoir; KHDB – Khamar-Daban Range. The black line at the top of the vertical sections shows the topography.

and gabbroids in the basement (Figs. 2–3). Outcrops of these rocks are located around the basin. The density of gabbro equals 2.9–3.1 g/cm^3. As a result of metamorphic and metasomatic transformations, garnet appears in gabbro in large quantities, its density being 3.60–4.30 g/cm^3 (pyrope – 3.57; almandine – 4.30; grossular – 3.60). This fact significantly increases the density of the gabbros transformed into eclogite-like rocks. Metagabbro and eclogite-like rocks are among gneisses and schists with a density of about 2.7 g/cm^3. A significant difference in the densities of gabbro, metagabbro and host rocks might have been decisive in the formation of the Baikal structure; at its bottom there are three rift-induced basins separated by uplifts (Fig. 2). The middle basin is the most structurally pronounced one: it largely corresponds to the location of dense gabbro-metagabbro rocks (Figs. 2, 3). As a result of the regional Cenozoic compression that led to leftward displacements within the Olkhon strike-slip zone, a pull-apart structure is likely to have formed, which inherited the ancient structure of the tectonic layering in the Olkhon zone. Within its limits, stemming from strike-slip displacements, heavy bodies of gabbro-metagabbro contributed to the subsidence of the Earth's crust segments with the formation of the basins.

Based on active seismic data, the research of Nielsen and Thybo (2009) denoted a 10 km thick sedimentary sequence under Baikal. The presence of the large sedimentary cover is also apparent in our acquired models. In the horizontal section of the S-velocity anomalies at 5 km depth (Fig. 5), the Middle Baikal basin stands out as a low-velocity linear anomaly. By contrast, the sediments of the South Baikal basin are not so distinct. Perhaps this is because the southern part of Baikal in the region of the Khamar-Daban Range has a low ray density, which can be observed in Fig. 4 and is also confirmed by the checkerboard test in Fig. 7. In addition, the high-amplitude high-velocity anomaly observed in the Irkutsk Reservoir area 'suppresses' a potential low-velocity anomaly in the upper part of the section, related to the sedimentary sequence of the South Baikal basin.

This assumption is proved by the synthetic test with realistic anomalies in Fig. 8. Therefore, a synthetic test was carried out to determine the resolution of the sedimentary cover recovery beneath Lake Baikal (Fig. 8). In this test, we set a 10 km thick sedimentary layer under Lake Baikal and a high-velocity anomaly in the Irkutsk Reservoir area. Following the test results, the expected low-velocity anomaly of the sedimentary cover in the South Baikal basin is not discerned. It may be due to the presence of a high-velocity high-intensity anomaly, which suppresses the anomaly associated with deposits under Baikal. The other anomalies are well resolved. Among them are the near-surface high-velocity ones under Baikal and near the Irkutsk Reservoir, large low-velocity one related to the BRZ, and high-velocity anomaly associated with the Siberian Craton.

4.3. The BRZ formation

Rift processes in the BRZ began about 30 Ma ago, which coincided with the most active phase of the collision of the Indian Plate with Eurasia. This is one of the most important arguments in favor of the fact that it was this collision and subsequent interplate movements that played a decisive role in the emergence of the Baikal Rift (passive rift model). On the other hand, the presence of areas with active volcanism in some parts of the BRZ indicates that mantle processes also play a certain role in the implementation of rifting processes (active rift model). Next, we consider in more detail the arguments for and against the active and passive models.

Arguments for and against the active theory:

1. The BRZ occupies the so-called Sayan-Baikal uplift, which reaches a level of 3000 m above sea level on the flanks, and up to 1500 m in the central zone. Proponents of the active rift model use this fact to prove the presence of an anomalous mantle under the BRZ.
2. Logachev (2005) noted that the inheritance of modern rift processes from older structures is far from being traced everywhere. Thus, in the region of the Muya 'microcontinent', the BRZ comes across the structure and the folded belt, and even invades the eastern flank of

the Archean Aldan Shield. This discrepancy is considered by some authors as an argument in favor of the active rift model.

3. Subsequent to the deep seismic sounding results, anomalously low velocities are observed under the crust in the area of Lake Baikal (Krylov et al., 1981; Suvorov et al., 1999, etc.). This is assumed to indicate the presence of an anomalous mantle (asthenosphere) directly at the base of the crust under Baikal. According to these data, the crustal thickness in the BRZ cross varies insignificantly within 35–40 km. We can say that, in general, these results also confirm the active rift model. However, this conclusion is refuted by the receiver function analysis (Zorin et al., 2002, Gao et al., 2004): along the profile from the Siberian Craton to the southeast, through the southern part of Baikal, and after a slight thinning of the crust, its strong thickening occurs under Baikal up to 55 km under Transbaikalia. The layer that was interpreted as the 'anomalous mantle' is represented in these models by the high-velocity lower part of the crust. In addition, exactly the same residuals could be caused by crustal variations, which follow from (Zorin et al., 2002).

The results of the current work show that on profiles AA', BB' and DD' (Fig. 6), along the axis of the Southern and Middle Baikal block, a jump in the lower boundary of the low-velocity anomaly is also clearly visible. In addition, under the southeastern part of the BRZ, there is an increase in the thickness of the low-velocity anomaly, which can be interpreted as a growth in the thickness of the crust. This can be considered as an argument with a minus sign for the anomalous mantle under the BRZ and, accordingly, active rifting.

4. The results of teleseismic tomography (Gao et al., 1994, 2003; Tiberi et al., 2003, Zhao et al., 2006) demonstrate a low-velocity anomaly under the BRZ, which shifts under the Siberian Craton at great depths. This could be used as an argument in favor of active rifting, according to which the separation of the Baikal Rift occurs under the action of a plume that rises from under the craton. These results are confirmed by tomographic models (Kulakov, 2008) obtained using global and regional data for a much larger area. However, the Baikal Basin in these models, where the maximum displacement is observed, does not coincide with the maximum intensity of the low-velocity anomalies. This shows a weak relationship between the distribution of the anomalous mantle and extension regions. In addition, according to our results, the low seismic velocities in the entire crust under the Eastern Sayan (profiles AA' and CC', Fig. 6) were interpreted as the result of the influence of a mantle plume, whose heat flow heats up the crust. If a geological object characterized by high temperatures (a mantle plume or an asthenospheric diapir) were present under Lake Baikal, then, most likely, its influence would similarly manifest itself in seismic tomography models of the crust. However, according to the profiles BB' and DD' (Fig. 6), the lower boundary of the low-velocity anomaly is clearly visible. Thus, it points to the absence of a plume or diapir directly under Lake Baikal, which is an argument against the active theory.
5. The area of low-velocity anomalous mantle at depths of 50–150 km in the models of Kulakov, (2008), as well as the low-velocity anomaly under the Eastern Sayan in this work, ideally coincide with the distribution of the Cenozoic volcanism. The presence of basaltic Cenozoic volcanism in the BRZ could be used as an argument for active rifting. However, its distribution over the area does not coincide with the BRZ position (Fig. 2). More specifically, the plume magmatism of the Eastern Sayan is localized west of the BRZ and is characterized by a large manifestation of the Late Cenozoic magmatic fields (Kiselev et al., 1978; Rasskazov et al., 2002). This magmatism belongs to the Khubsugul plume (Dobretsov, 2020; Yarmolyuk et al., 2013), whose deep structure is shown in seismic azimuthal anisotropy and gravity data (Gao et al., 1994; Zorin et al., 2003).
6. The BRZ is characterized by an increased heat flow. However, according to Golubev (2007), the local heat flow anomalies are confined to the fault zones and are associated with convective heat transfer. According to the latest results on regional spectral analysis of the lithospheric geomahnetic field, resulted in a distribution of the depth to the bottom of the lithospheric magnetic sources (Filippova et al., 2021), the mean heat flow values differ little from those at the Siberian Platform. Moreover, they are lower than in Transbaikalia.
7. The thick crust that existed in the pre-rift time in the Amur-Mongolian Plate at the contact with the Siberian Craton (Zorin et al., 2002, Gao et al., 2004) explains the localization of the fault zone in the area of Lake Baikal. As shown by the results of numerical modeling for the Dead Sea Region (Sobolev et al., 2005), the most probable place for the formation of ruptures in the lithosphere coincides with the greatest thickness of the crust. This suggests that the opening of the Baikal Rift did not require additional heating of the lithosphere, which is assumed by the concept of active rifting.

Arguments for and against the passive theory:

1. The beginning of rifting processes in the Baikal Region 30 Ma coincided with the most active phase of the collision of Hindustan with Eurasia, which speaks in favor of the passive model.
2. The capability of implementing the passive rifting mechanism in the BRZ due to the movement of lithospheric plates resulting from the collision of India and the subduction of the Pacific Plate has been shown by many numerical (see, e.g., Flesch et al., 2001; Holt et al., 2000) and analogue experiments (Peltzer and Tapponnier, 1988; Chemenda et al., 2002). We are not aware of any numerical or physical experiments that would show the opening of the Baikal Rift solely due to mantle uplift and would confirm the active rifting concept.
3. The high-velocity blocks in the region of Olkhon Island, located within the central block of Baikal, which we interpreted as high-density gabbro-metagabbro bodies, indicates that the compression zone probably shifted in the region. It led to left-sided displacements with the formation of pull-apart structures. This might have occurred in the Cenozoic due to the long-range impact of the Indo-Eurasian collision.

The strong ledge of the Siberian Craton played a key role in the formation of the extension region around Lake Baikal (Fig. 1). As shown by the results of GPS observations (Calais et al., 2003), summarized in the form of a simplified diagram in Fig. 9, and by numerical simulations (e.g. Flesch et al., 2001; Holt et al., 2000), the collision of the Indian Plate leads to deformation of the entire folded region up to the Siberian Craton. If in the southern part of this area the displacement vectors have a northerly direction, then in the northern part they tend to the northeast. The presence of the ledge of the Siberian Craton during the northeast displacement of the lithosphere in the Amur-Mongolian block leads to the formation of a 'pocket' behind the craton, where tensile deformations are manifested.

The concentration of tensile deformations at the boundary of the Siberian Craton may be explained by structural inhomogeneities of the crust and lithosphere. Following the assumptions made in Zorin et al., (2003), in the pre-rift time at the junction of the Siberian Plate in the place of present-day Lake Baikal, there existed a sharp contrast in the thickness of the crust: 30–35 km under the craton and 45–55 km under the folded area. This contrast is explained by the process of crustal compression in the earlier stages of the region's development. The results of mathematical modeling (see, for example, Sobolev et al., 2005) indicate that the regions with the greatest crustal thickness have the least strength of the lithosphere. If we add here the contrast in the thickness of the lithosphere between the craton and the Amur-Mongolian block (Zorin et al., 1990), then it becomes obvious that the part of the folded area bordering the craton is the most probable place for the localization of tensile deformations. Based on this assumption, no additional heating of this region by the anomalous mantle is required for

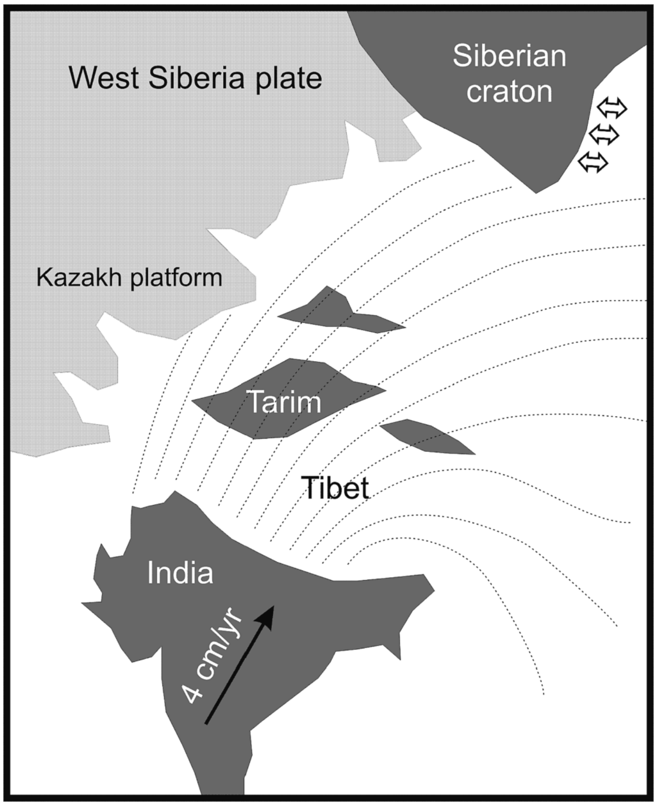

Fig. 9. Simplified diagram of lithospheric motion in the Central Asian Fold Belt caused by the Indian Plate (simplified generalization of GPS data from Calais et al., 2003). The dashed lines indicate the direction of movement. One can see that when the Siberian Craton is immobile, tensile deformations should appear behind its ledge.

its weakening and extension.

Based on all the above facts, we are inclined towards the passive model regarding the formation of the Baikal Rift. The main argument for us against the active rifting concept is the discrepancy between the activity of the processes of lithospheric expansion and the location of the anomalous mantle. The maximum intensity of low-velocity anomalies both in the crust and in the mantle is observed south of the Siberian Craton, which is consistent with manifestations of the Cenozoic magmatism. At the same time, the maximum intensity of rifting processes is observed in the Lake Baikal basin, under which mantle anomalies are much less significant and volcanism is completely absent. Hence, we assume the opening of the Baikal basin to have occurred exclusively due to interplate interactions.

At the same time, we are ready to accept that in the formation of small rift valleys south of the Siberian Craton, an active rifting mechanism might have taken place. The anomalous mantle could have warmed up the lithosphere, which led to a weakening of its strength, resulting in the formation of meridional extension zones in a perpendicular direction relative to the general compression trend from the Indian Craton.

5. Conclusions

The Baikal Rift Zone and adjacent territories were scrutinized through seismic tomography with data from local seismological networks. The models have a good resolution in the Baikal region and a sufficient resolution in surrounding areas, which made it possible to reveal the regularities of their deep structure.

According to the data obtained, we revealed the following features of the structure of the Earth's upper crust in the BRZ and surrounding territories:

a. The Baikal Rift Zone is characterized by a low-velocity anomaly whose lower boundary can be traced back to a depth of 35–50 km, which is in accord with contemporary ideas on the Moho discontinuity depth. In addition, under the South and Middle Baikal blocks there is a thinning of the low-velocity anomaly, which corresponds to the Moho jump scrutinized by Zorin et. al., 2003. This indicates a thinning of the low-velocity anomaly, which may also be evidence of crustal thinning.
b. The Siberian Craton within the study area is manifested as a high-velocity anomaly, which is indicative of its being a dense monolithic block.
c. There exists a large low-velocity anomaly under the Eastern Sayan, which is apparently due to the influence of the Cenozoic plume heating up the crust and thereby causing a slowdown in seismic velocities in the crust.
d. Under the Middle Baikal basin, in the vicinity of Olkhon Island, we observe high-velocity anomalies. These anomalies are assumed to be due to the presence of high-density gabbro and metagabbro rocks. As a consequence of regional compression that led to the formation of the Cenozoic leftward displacements within the Early Paleozoic Olkhon strike-slip zone, a pull-apart structure is likely to have formed. This could have happened due to the long-range impact of the Indo-Eurasian collision.
e. In the Irkutsk Reservoir area over the Siberian Craton, we single out an isometric high-velocity anomaly with a diameter of about 50 km and reaching a depth of ~ 30 km. The anomaly is thought to be associated with the manifestation of igneous rocks similar to the Late Permian–Early Triassic Chadobets alkaline-carbonatite complex that is close in shape and size.

Pursuant to the results obtained in our research, as well as on the basis of the review of the existing works, we are inclined towards the passive model for the formation of the Baikal Rift. The main argument against the concept of active rifting seems to be the discrepancy between the activity of the lithospheric extension processes and the location of the anomalous mantle.

Declaration of Competing Interest

The authors declare that they have no known competing financial interests or personal relationships that could have appeared to influence the work reported in this paper.

Data availability

The authors do not have permission to share data.

Acknowledgements

The studies were carried out within research projects of NSU, IPGG SB RAS, IGM SB RAS and IZMIRAN. The work was supported by the Ministry of Education and Science of Russia. The data used in the work were obtained with large-scale research facilities «Seismic infrasound array for monitoring Arctic cryolitozone and continuous seismic monitoring of the Russian Federation, neighbouring territories and the world». The work on data processing was supported by the state assignment according to the research project AAAA-A19-119011490129-0.

The work on overview of geology was supported by RFBR grant No. 19-35-60002. The work on seismic tomography of the region was supported by the state assignment according to the research project FSUS-2022-0019. The work on interpretation of the results was supported by the state assignment according to the research project FWZZ-2022-0017.

We are very grateful to Kelly Liu and Vineet Kumar Gahalaut for the very constructive reviews, which helped us to improve the paper.

References

Artyushkov, E.V., 1993. Physical tectonics. Nauka, Moscow 1–456 in Russian.

Bazarov, D. B., 1986. The Cenozoic of the Baikal and western Trans-Baikal regions. Novosibirsk, 180 (in Russian).

Buslov, M.M., 2012. Geodynamic nature of the Baikal Rift Zone and its sedimentary filling in the Cretaceous–Cenozoic: the effect of the far-range impact of the Mongolo-Okhotsk and Indo-Eurasian collisions. Russ. Geol. Geophys. 53 (9), 955–962. https://doi.org/10.1016/j.rgg.2012.07.010.

Buslov, M.M., De Grave, J., Bataleva, E.A.V., Batalev, V.Y., 2007. Cenozoic tectonic and geodynamic evolution of the Kyrgyz Tien Shan Mountains: A review of geological, thermochronological and geophysical data. J. Asian Earth Sci. 29 (2–3), 205–214.

Buslov, M.M., Kokh, D.A., De Grave, J., 2008. Mesozoic-Cenozoic tectonics and geodynamics of Altai, Tien Shan, and Northern Kazakhstan, from apatite fission-track data. Russ. Geol. Geophys. 49 (9), 648–654.

Calais, E., Vergnolle, M., San'Kov, V., Lukhnev, A., Miroshnitchenko, A., Amarjargal, S., Déverchère, J., 2003. GPS measurements of crustal deformation in the Baikal-Mongolia area (1994–2002): Implications for current kinematics of Asia. J. Geophys. Res. Solid Earth 108 (B10), 1–13. https://doi.org/10.1029/2002JB002373.

Chebotarev, D.A., Doroshkevich, A.G., Sharygin, V.V., Yudin, D.S., Ponomarchuk, A.V., Sergeev, S.A., 2017. Geochronology of the Chuktukon carbonatite massif, Chadobets uplift (Krasnoyarsk Territory). Russ. Geol. Geophys. 58 (10), 1222–1231.

Chemenda, A., Déverchère, J., Calais, E., 2002. Three-dimensional laboratory modelling of rifting: application to the Baikal Rift. Russia. Tectonophysics 356 (4), 253–273.

Davy, P., Cobbold, P.R., 1988. Indentation tectonics in nature and experiment. 1. Experiments scaled for gravity. Bull. Geol. Inst. Univ. Uppsala 14, 129–141.

De Grave, J., Buslov, M.M., 2007. Distant effects of India-Eurasia convergence and Mesozoic intracontinental deformation in Central Asia: Constraints from apatite fission-track thermochronology. J. Asian Earth Sci. 29 (2–3), 188–204.

Delvaux, D., Moeys, R., Stapel, G., Petit, C., Levi, K., Miroshnichenko, A., Ruzhich, V., Sankov, V., 1997. Paleostress reconstructions and geodynamics of the Baikal region, central Asia, Part 2. Cenozoic rifting. Tectonophysics 282 (1–4), 1–38.

Déverchère, J., Petit, C., Gileva, N., Radziminovitch, N., Melnikova, V., Sankov, V., 2001. Depth distribution of earthquakes in the Baikal rift system and its implications for the rheology of the lithosphere. Geophys. J. Int. 146 (3), 714–730. https://doi.org/10.1046/j.0956-540X.2001.1484.484.x.

Dobretsov, N.L., 2020. Interaction of plate tectonics and plume tectonics: probable models and typical examples. Russ. Geol. Geophys. 61 (5–6), 617–647 in Russian). 10.15372/gig2020102.

Dobretsov, N.L., Berzin, N.A., Buslov, M.M., 1995. Opening and tectonic evolution of the Paleo-Asian Ocean. Int. Geol. Rev. 37 (4), 335–360.

Dobretsov, N.L., Buslov, M.M., Delvaux, D., Berzin, N.A., Ermikov, V.D., 1996. Meso-and Cenozoic tectonics of the Central Asian mountain belt: effects of lithospheric plate interaction and mantle plumes. Int. Geol. Rev. 38 (5), 430–466.

Dobretsov, N., Buslov, M.M., De Grave, J., Sklyarov, E.V., 2013. Interplay of magmatism, sedimentation, and collision processes in the Siberian craton and the flanking orogens. Russ. Geol. Geophys. 54 (10), 1135–1149.

Dobretsov, N.L., Buslov, M.M., Vasilevsky, A.N., Vetrov, E.V., Nevedrova, N.N., 2016. Cenozoic history of topography in southeastern Gorny Altai: thermochronology and resistivity and gravity records. Russ. Geol. Geophys. 57 (11), 1525–1534.

Dobretsov, N.L., Buslov, M.M., Vasilevsky, A.N., 2019. Geodynamic complexes and structures of Transbaikalia: record in gravity data. Russ. Geol. Geophys. 60 (3), 301–317 in Russian.

Dobretsov, N.L., Metelkin, D.V., Vasilevskiy, A.N., 2021. Typical characteristics of the earth's magnetic and gravity fields related to global and regional tectonics. Russ. Geol. Geophys. 62 (1), 10–30 in Russian.

Donskaya, T.V., Gladkochub, D.P., Fedorovsky, V.S., Sklyarov, E.V., Cho, M., Sergeev, S. A., Demonterova, E.I., Mazukabzov, A.M., Lepekhina, E.N., Cheong, W., Kim, J., 2017. Pre-collisional (> 0.5 Ga) complexes of the Olkhon terrane (southern Siberia) as an echo of events in the Central Asian Orogenic Belt. Gondw. Res. 42, 243–263.

Duchkov, A.D., Sokolova, L. S., 2014. The heat flow of Siberia. All-Russian conference "Geophysical methods of studying the Earth's crust" dedicated to the 100th anniversary of the birth of Academician NN Puzyrev. IPGG SB RAS, Novosibirsk, 211-216 (in Russian).

Fedorovskii, V.S., Mazukabzov, A.M., Sklyarov, E.V., Gladkochub, D.P., Donskaya, T.V., Lavrenchuk, A.V., 2019. Olkhon terraine - phantom or reality? In Geodynamic Evolution of the Lithosphere of the Central Asian Mobile Belt (from ocean to continent). Irkutsk 271–272 in Russian.

Fedorovsky, V.S., Sklyarov, E.V., 2015. The Olkhon geodynamic proving ground (Lake Baikal): high resolution satellite data and geological maps of new generation. Geodynamics & Tectonophysics 1 (4), 331–418.

Fedorovsky, V.S., Donskaya, T.V., Gladkochub, D.P., Khromykh, S.V., Mazukabzov, A.M., Mekhonoshin, A.S., Yudin, D.S., 2005. The Ol'khon collision system (Baikal region). In: Structural and tectonic correlation across the Central Asia orogenic collage: northeastern segment (Guidebook and abstract volume of the Siberian Workshop IGCP-480)/Ed. EV Sklyarov. IEC SB RAS, Irkutsk, pp. 3–76 in Russian.

Fedorovsky, V.S., Sklyarov, E.V., Izokh, A.E., Kotov, A.B., Lavrenchuk, A.V., Mazukabzov, A.M., 2010. Strike-slip tectogenesis and alkaline-mafic magmatism in the collision system of the Caledonides of the Western Baikal region. Geol. Geophys. 51 (5), 682–700. https://doi.org/10.1016/j.rgg.2010.04.009.

Fedorvoskii, V.S., Vladimirov, A.G., Khain, E.V., Kargopolov, S.A., Gibsher, A.S., Izokh, A.E., 1995. Tectonics, metamorphism, and magmatism of collision zones of the Caledonides in Central Asia. Geotektonika 3–22 in Russian.

Filippova, A.I., Golubev, V.A., Filippov, S.V., 2021. Curie Point Depth and Thermal State of the Lithosphere Beneath the Northeastern Flank of the Baikal Rift Zone and Adjacent Areas. Surv. Geophys. 42 (5), 1143–1170. https://doi.org/10.1007/s10712-021-09651-7.

Flesch, L.M., Haines, A.J., Holt, W.E., 2001. Dynamics of the India-Eurasia collision zone. J. Geophys. Res. Solid Earth 106 (B8), 16435–16460. http://doi.wiley.com/10.1029/2001JB000208.

Fournier, M., Jolivet, L., Huchon, P., Sergeyev, K.F., Oscorbin, L.S., 1994. Neogene strike-slip faulting in Sakhalin and the Japan Sea opening. J. Geophys. Res. Solid Earth 99 (B2), 2701–2725.

Fournier, M., Bellahsen, N., Fabbri, O., Gunnell, Y., 2004. Oblique Rifting and Segmentation of the NE Gulf of Aden Passive Margin. Geochemistry, Geophysics, Geosystems 5 (11), 1–24.

Gao, S., Davis, P.M., Liu, H., Slack, P.D., Zorin, Y.A., Mordvinova, V.V., Meyer, R.P., 1994. Seismic anisotropy and mantle flow beneath the Baikal rift zone. Nature 371 (6493), 149–151. https://doi.org/10.1038/371149a0.

Gao, S.S., Liu, K.H., Davis, P.M., Slack, P.D., Zorin, Y.A., Mordvinova, V.V., Kozhevnikov, V.M., 2003. Evidence for small-scale mantle convection in the upper mantle beneath the Baikal rift zone. J. Geophys. Res. Solid Earth 108 (B4). http://doi.wiley.com/10.1029/2002JB002039.

Gao, S.S., Liu, K.H., Chen, C., 2004. Significant crustal thinning beneath the Baikal rift zone: New constraints from receiver function analysis. Geophys. Res. Lett. 31 (20) https://doi.org/10.1029/2004GL020813.

Gileva, N.A., Melnikova, V.I., Radziminovich, N.A., Deverchbre, J., 2000. Location of earthquakes and average velocity parameters of the crust in some areas of the Baikal region. Russ. Geol. Geophys. 41 (5), 609–615 in Russian.

Golenetsky, S.I., Perevalova, G.I., 1988. On the use of computers in the summary processing of observations of a local network of seismic stations in the Baikal zone. Research on the Search for earthquake precursors in Siberia 99–108 in Russian.

Golubev, V. A., 2007. Conductive and convective heat transfer in the Baikal Rift Zone. Geo, Novosibirsk, 222 (in Russian).

Holt, W.E., Chamot-Rooke, N., Le Pichon, X., Haines, A.J., Shen-Tu, B., Ren, J., 2000. Velocity field in Asia inferred from Quaternary fault slip rates and Global Positioning System observations. J. Geophys. Res. Solid Earth 105 (B8), 19185–19209.

Hutchinson, D.R., Golmshtok, A.J., Zonenshain, L.P., Moore, T.C., Scholz, C.A., Klitgord, K.D., 1992. Depositional and tectonic framework of the rift basins of Lake Baikal from multichannel seismic data. Geology 20 (7), 589–592.

Jolivet, M., Arzhannikov, S., Chauvet, A., Arzhannikova, A., Vassallo, R., Kulagina, N., Akulova, V., 2013. Accommodating large-scale intracontinental extension and compression in a single stress-field: a key example from the Baikal Rift System. Gondw. Res. 24 (3–4), 918–935.

Jolivet, L., Davy, P., Cobbold, P., 1990. Right-lateral shear along the northwest Pacific margin and the India-Eurasia collision. Tectonics 9 (6), 1409–1419.

Jolivet, L., Fournier, M., Huchon, P., Rozhdestvenskiy, V.S., Sergeyev, K.F., Oscorbin, L. S., 1992. Cenozoic intracontinental dextral motion in the Okhotsk-Japan Sea Region. Tectonics 11 (5), 968–977.

Kimura, G., Takahashi, M., Kono, M., 1990. Mesozoic collision—Extrusion tectonics in eastern Asia. Tectonophysics 181 (1–4), 15–23.

Kiselev, A.I., Golovko, H.A., Medvedev, M.E., 1978. Petrochemistry of Cenozoic basalts and associated rocks in the Baikal rift zone. Tectonophysics 45 (1), 49–59.

Koulakov, I., 2009. LOTOS code for local earthquake tomographic inversion: Benchmarks for testing tomographic algorithms. Bull. Seismol. Soc. Am. 99 (1), 194–214. https://doi.org/10.1785/0120080013.

Koulakov, I., Tychkov, S., Bushenkova, N., Vasilevsky, A., 2002. Structure and dynamics of the upper mantle beneath the Alpine-Himalayan orogenic belt, from teleseismic tomography. Tectonophysics 358 (1–4), 77–96. https://doi.org/10.1016/S0040-1951(02)00418-3.

Koulakov, I., Maksotova, G., Mukhopadhyay, S., Raoof, J., Kayal, J.R., Jakovlev, A., Vasilevsky, A., 2014. Variations of the crustal thickness in Nepal Himalayas based on tomographic inversion of regional earthquake data. Solid Earth Discuss. 6 (2).

Krylov, S. V., Mandelbaum, M. M., Mishenkin, B. P., Mishenkina, Z. R., Petrik, G. V., Seleznev, B. S., 1981. The Baikal interior (from seismic data). Nauka 105 (in Russian).

Kulakov, I.Y., 1999. Three-dimensional seismic heterogeneities beneath the Baikal region according to data of local teleseismic tomography. Russ. Geol. Geophys. 40 (3), 317–331.

Kulakov, I.Y., 2008. Upper mantle structure beneath southern Siberia and Mongolia, from regional seismic tomography. Russian Geology and Geophysics 49 (3), 187–196. https://doi.org/10.1016/j.rgg.2007.06.016.

Laske, G., Masters, G., Ma, Z., Pasyanos, M., 2013. Update on CRUST1. 0—A1-degree global model of Earth's crust. In. Geophys. Res. Abstr. 15, 2658.

Lebedev, S., Meier, T., van der Hilst, R.D., 2006. Asthenospheric flow and origin of volcanism in the Baikal Rift area. Earth Planet. Sci. Lett. 249 (3–4), 415–424.

Lesne, O., Calais, E., Deverchère, J., Chéry, J., Hassani, R., 2000. Dynamics of intracontinental extension in the north Baikal rift from two-dimensional numerical deformation modeling. J. Geophys. Res. Solid Earth 105 (B9), 21727–21744.

Levi, K.G., Babushkin, S.M., Badardinov, A.A., Buddo, V.Y., Larkin, G.V., Miroshnichenko, A.I., San'kov, V.A., Ruzhich, V.V., Wong, H.K., Delvau, D., Colman, S., 1995. Active Baikal tectonics. Russ. Geol. Geophys. 36 (10), 143–154.

Levi, K.G., Miroshnichenko, A.I., San'kov, V.A., Babushkin, S.M., Larkin, G.V., Badardinov, A.A., Wong, H.K., Colman, S., Delvaux, D., 1997. Active faults of the Baikal depression. Bull. Centres Rech. Explor. Prod. Elf-Aquitaine 21 (2), 399–434.

Logachev, N.A., 1999. Main structural features and geodynamics of the Baikal rift zone. Phys. Mesomech. 2 (1–2), 163–170 in Russian.

Logachev, N.A., 2003. History and geodynamics of the Baikal rift. Russ. Geol. Geophys. 44 (5), 391–406.

Logachev, N.A., 2005. History and geodynamics of the Baikal rift, in: Goldin, S.V., Mazukabzov, A.M., Seleznev, V.S. (Eds.), Actual Problems of Modern Geodynamics of Asia [in Russian]. Izd. SO RAN, Novosibirsk, pp. 9–32. Logachev, N.A., Rasskazov, S.V., Ivanov, A.V., Levi, K.G., Bukharov, A.A., Kashik, S.A., Sherman, S.I., 1996. Cenozoic rifting in continental lithosphere, in: Logachev, N.A. (Ed.), Lithosphere of Central Asia [in Russian], Nauka, Novosibirsk, pp. 57–80.

Logatchev, N.A., Zorin, Y.A., 1987. Evidence and causes of the two-stage development of the Baikal rift. Tectonophysics 143 (1–3), 225–234.

Lukhnev, A.V., Sankov, V.A., Miroshnichenko, A.I., Ashurkov, S.V., Calais, E., 2010. GPS rotation and strain rates in the Baikal-Mongolia region. Russ. Geol. Geophys. 51 (7), 785–793 in Russian.

Lunina, O.V., Gladkov, A.S., Sherstyankin, P.P., 2010. A new electronic map of active faults for southeastern Siberia. In Doklady Earth Sciences 433 (2), 1016–1021.

Lysak, S.V., 1984. Terrestrial heat flow in the south of East Siberia. Tectonophysics 103 (1–4), 205–215.

Mashchuk, I.M., Akulov, N.I., 2012. Oligocene deposits of the Baikal rift valley. Russ. Geol. Geophys. 53 (4), 356–366. https://doi.org/10.1016/j.rgg.2012.02.012.

Medved, I., Koulakov, I., Mukhopadhyay, S., Jakovlev, A., 2022. Lithosphere Structure in the Collision Zone of the NW Himalayas Revealed by Local Earthquake Tomography. J. Geodyn. 101922 https://doi.org/10.1016/j.jog.2022.101922.

Melnikova, V.I., Gileva, N.A., Radziminovich, N.A., Masalskii, O.K., Chechelnitskii, V.V., 2010. Seismicity of the Baikal Rift Zone for the digital recording period of earthquake observation (2001–2006). Seismic Instruments 46 (2), 138–151. https://doi.org/10.3103/s0747923910020076.

Molnar, P., Tapponnier, P., 1975. Cenozoic tectonics of Asia: effects of a continental collision. Science 189 (4201), 419–426.

Mordvinova, V. V., Kobelev, M. M., Chritova, M. A., Turutanov, E. Ch., Kobeleva, E. A., Trynkova, D. S., Tsydypova, L. R., 2019. Deep velocity structure of the southern edge of the Siberian craton and Baikal rifting. In Doklady Earth Sciences 484(1), 93-97 (in Russian). 10.31857/S0869-5652484193-97.

Mordvinova, V.V., Vinnik, L.P., Kosarev, G.L., Oreshin, S.I., Treusov, A.V., 2000. Teleseismic tomography of the Baikal rift lithosphere. In Doklady Earth Sciences 372, 716–720.

Nielsen, C., Thybo, H., 2009. No Moho uplift below the Baikal Rift Zone: Evidence from a seismic refraction profile across southern Lake Baikal. J. Geophys. Res. Solid Earth 114 (B8).

Nikolaev, A.V., Sanina, I.A., Trifonov, V.G., Vostrikov, G.A., 1985. Structure and evolution of the Pamir—Hindu Kush region lithosphere. Phys. Earth Planet. In. 41 (2–3), 199–206. https://doi.org/10.1016/0031-9201(85)90034-2.

Nolet, G., (Ed.),, 1987. Seismic tomography: With applications in global seismology and exploration geophysics Vol. 5. https://doi.org/10.1007/978-94-009-3899-1_1.

Paige, C.C., Saunders, M.A., 1982. LSQR: An algorithm for sparse linear equations and sparse least squares. ACM Transactions on Mathematical Software (TOMS) 8 (1), 43–71. https://doi.org/10.1145/355984.355989.

Peltzer, G., Tapponnier, P., 1988. Formation and evolution of strike-slip faults, rifts, and basins during the India-Asia collision: An experimental approach. J. Geophys. Res. Solid Earth 93 (B12), 15085–15117.

Petit, C., Burov, E., Tiberi, C., 2008. Strength of the lithosphere and strain localisation in the Baikal rift. Earth Planet. Sci. Lett. 269 (3–4), 523–529.

Petit, C., Deverchere, J., 2006. Structure and evolution of the Baikal rift: a synthesis. Geochem. Geophys. Geosyst. 7 (11), 1–26.

Petit, C., Deverchere, J., Houdry, F., Sankov, V.A., Melnikova, V.I., Delvaux, D., 1996. Present-day stress field changes along the Baikal rift and tectonic implications. Tectonics 15 (6), 1171–1191.

Petit, C., Koulakov, I., Deverchère, J., 1998. Velocity structure around the Baikal rift zone from teleseismic and local earthquake traveltimes and geodynamic implications. Tectonophysics 296 (1–2), 125–144. https://doi.org/10.1016/S0040-1951(98)00140-1.

Radziminovich, N.A., 2010. Focal depths of earthquakes in the Baikal region: a review. Izv. Phys. Solid Earth 46 (3), 216–229 in Russian.

Rasskazov, S.V., Sherman, S.I., Levi, K.G., Ruzhich, V.V., Kozhevnikov, V.M., Sankov, V. A., 2010. Academician N.A. Logatchev and his scientific school: contrubition to studies of the cenozoic continental rifting. Geodynamics & Tectonophysics 1(3), 209–224. (in Russian). 10.5800/GT-2010-1-3-0017.

Rasskazov, I.Y., Saksin, B.G., Petrov, V.A., Shevchenko, B.F., Usikov, V.I., Gil'manova, G. Z., 2014. Present-day stress-strain state in the upper crust of the Amurian lithosphere plate. Izv. Phys. Solid Earth 50 (3), 444–452. https://doi.org/10.1134/S1069351314030082.

Rasskazov, S.V., Saranina, E.V., Demonterova, E.I., Maslovskaya, M.N., Ivanov, A.V., 2002. Mantle components in Late Cenozoic volcanics of the East Sayan (from Pb, Sr, and Nd isotopes). Russ. Geol. Geophys. 43 (12), 1065–1079.

Rasskazov, S.V., Yasnygina, T.A., Chuvashova, I.S., Mikheeva, E.A., Snopkov, S.V., 2015. The Kultuk Volcano: spatial-temporal change of magmatic sources at the western terminus of the South Baikal basin between 18 and 12 Ma. Geodynamics & Tectonophysics 4 (2), 135–165.

Scholz, C.A., Klitgord, K.D., Hutchinson, D.R., Ten Brink, U.S., Zonenshain, L.P., Golmshtok, A.Y., Moore, T.C., 1993. Results of 1992 seismic reflection experiment in Lake Baikal. Eos Trans. AGU 74 (41), 465–470.

Seredkina, A.I., 2021. The state of the art in studying the deep structure of the earth's crust and upper mantle beneath the Baikal Rift from seismological data. Izv. Phys. Solid Earth 57 (2), 180–202. https://doi.org/10.31857/S0002333721020113 in Russian.

Seredkina, A., Kozhevnikov, V., Melnikova, V., Solovey, O., 2016. Seismicity and S-wave velocity structure of the crust and the upper mantle in the Baikal rift and adjacent regions. Phys. Earth Planet. In. 261, 152–160.

Sklyarov, E. V., Lavrenchuk, A. V., Fedorovsky, V. S., Gladkochub, D. P., Donskaya, T. V., Kotov, A. B., Mazukabzov, A. M., Starikova, A. E., 2020. Regional, Contact Metamorphism and Autometamorphism in the Olkhon Terrain (West Baikal Area). Petrology 28(1), 47–61. (in Russian). 10.1134/S0869591120010051.

Sobolev, S.V., Petrunin, A., Garfunkel, Z., Babeyko, A.Y., 2005. Thermo-mechanical model of the Dead Sea Transform. Earth Planet. Sci. Lett. 238 (1–2), 78–95. https://doi.org/10.1016/j.epsl.2005.06.058.

Song, Y., Krylov, S.V., Yang, B., Cai, L., Dong, S., Liang, T., Li, J., Xu, X., Mishenkina, Z. R., Petrik, G.V., Shelud'ko, I.F., Seleznev, V.S., Solov'ev, V.M., 1996. Deep seismic sounding of the lithosphere on the Baikal-Northeast China international transect. Geol. Geophys. 37 (2), 1–13.

Suvorov, V.D., Mishenkina, Z.R., Petrik, G.V., Sheludko, I.F., 1999. Earth's crust and its isostatic state in the Baikal Rift Zone and adjacent areas according to DSS data. Russ. Geol. Geophys. 40 (3), 304–316 in Russian.

Suvorov, V.D., Mishenkina, Z.M., Petrick, G.V., Sheludko, I.F., Seleznev, V.S., Solovyov, V.M., 2002. Structure of the crust in the Baikal rift zone and adjacent areas from Deep Seismic Sounding data. Tectonophysics 351 (1–2), 61–74. https://doi.org/10.1016/S0040-1951(02)00125-7.

Suvorov, V.D., Tubanov, T.s., A., 2008. Distribution of local earthquakes in the crust beneath central Lake Baikal. Russ. Geol. Geophys. 49 (8), 611–620 in Russian.

Ten Brink, U.S., Taylor, M.H., 2002. Crustal structure of central Lake Baikal: Insights into intracontinental rifting. Journal of Geophysical Research: Solid. Earth 107 (B7), ETG-2.

Tiberi, C., Diament, M., Déverchère, J., Petit-Mariani, C., Mikhailov, V., Tikhotsky, S., Achauer, U., 2003. Deep structure of the Baikal rift zone revealed by joint inversion of gravity and seismology. J. Geophys. Res. Solid Earth 108 (B3).

Um, J., Thurber, C., 1987. A fast algorithm for two-point seismic ray tracing. Bull. Seismol. Soc. Am. 77 (3), 972–986. https://doi.org/10.1785/BSSA0770030972.

Vinnik, L.P., Oreshin, S.I., Tsydypova, L.R., Mordvinova, V.V., Kobelev, M.M., Khritova, M.A., Tubanov, Ts.A., 2017. Crust and mantle of the Baikal rift zone from P- and S-wave receiver functions. Geodynamics & Tectonophysics 8 (4), 695–709. https://doi.org/10.5800/GT-2017-8-4-0313.

Vladimirov, A.G., Mekhonoshin, A.S., Khromykh, S.V., Mikheev, E.I., Travin, A.V., Volkova, N.I., Kolotilina, T.B., Davydenko, Y.A., Borodina, E.V., Khlestov, V.V., 2017. Mechanisms of mantle-crust interaction at deep levels of collision orogens (case of the Olkhon region, West Pribaikalie). Geodynamics and Tectonophysics 8 (2), 223–268. https://doi.org/10.5800/GT-2017-8-2-0240.

Windley, B.F., Allen, M.B., 1993. Mongolian plateau: Evidence for a late Cenozoic mantle plume under central Asia. Geology 21 (4), 295–298.

Wu, H., Huang, Z., Zhao, D., 2021. Deep structure beneath the southwestern flank of the Baikal rift zone and adjacent areas. Phys. Earth Planet. In. 310, 106616 https://doi.org/10.1016/j.pepi.2020.106616.

Yakovlev, A.V., Koulakov, I.Y., Tychkov, S.A., 2007. Moho depths and three-dimensional velocity structure of the crust and upper mantle beneath the Baikal region, from local tomography. Russ. Geol. Geophys. 48 (2), 204–220.

Yarmolyuk, V.V., Kuzmin, M.I., Vorontsov, A.A., 2013. West pacific-type convergent boundaries and their role in the formation of the Central Asian fold belt. Russ. Geol. Geophys. 54 (12), 1831–1850 in Russian.

Zhao, D., Lei, J., Inoue, T., Yamada, A., Gao, S.S., 2006. Deep structure and origin of the Baikal rift zone. Earth Planet. Sci. Lett. 243 (3–4), 681–691. https://doi.org/10.1016/j.epsl.2006.01.033.

Zonenshain, L.P., Kazmin, V.G., 1995. Structure, Stages of Rifting, and Kinematics, Baikal Rift, Russia. In: Ojakangas, R.W., Dickas, A.B., Green, J.C. (eds) Basement Tectonics 10. Proceedings of the International Conferences on Basement Tectonics, vol 4. Springer, Dordrecht. 10.1007/978-94-017-0831-9_41.

Zonenshain, L.P., Golmshtok, A.Y., Hutchinson, D.R., 1992. Structure of the Baikal rift. Geotektonika 5, 63–77 in Russian.

Zorin, Y.A., 1981. The Baikal rift: an example of the intrusion of asthenospheric material into the lithosphere as the cause of disruption of lithospheric plates. Tectonophysics 73 (1–3), 91–104.

Zorin, Y.A., Mordvinova, V.V., Turutanov, E.K., Belichenko, B.G., Artemyev, A.A., Kosarev, G.L., Gao, S.S., 2002. Low seismic velocity layers in the Earth's crust beneath Eastern Siberia (Russia) and Central Mongolia: receiver function data and their possible geological implication. Tectonophysics 359 (3–4), 307–327. https://doi.org/10.1016/S0040-1951(02)00531-0.

Zorin, Y.A., Novoselova, M.R., Turutanov, E.K., Kozhevnikov, V.M., 1990. Structure of the lithosphere of the Mongolian-Siberian mountainous province. J. Geodyn. 11 (4), 327–342.

Zorin, Y.A., Turutanov, E.H., 2005. Plumes and geodynamics of the Baikal Rift zone. Geol. Geophys. 46 (7), 685–699.

Zorin, Y.A., Turutanov, E.K., Mordvinova, V.V., Kozhevnikov, V.M., Yanovskaya, T.B., Treussov, A.V., 2003. The Baikal rift zone: the effect of mantle plumes on older structure. Tectonophysics 371 (1–4), 153–173.